

Tunable Topologically-protected Super- and Subradiant Boundary States in One-Dimensional Atomic Arrays

Anwei Zhang¹, Xianfeng Chen^{1,2}, Vladislav V. Yakovlev³, and Luqi Yuan^{1,2,*}

¹*School of Physics and Astronomy,*

Shanghai Jiao Tong University, Shanghai 200240, China

²*State Key Laboratory of Advanced Optical Communication Systems and Networks,*

Shanghai Jiao Tong University, Shanghai 200240, China

³*Texas A&M University, College Station, Texas 77843, USA*

**Corresponding author: yuanluqi@sjtu.edu.cn*

Abstract

Single-photon super- and subradiance are important for the quantum memory and quantum information. We investigate one-dimensional atomic arrays under the spatially periodic magnetic field with a tunable phase, which provides a distinctive physics aspect of revealing exotic two-dimensional topological phenomena with a synthetic dimension. A butterfly-like nontrivial band-structure associated with the non-Hermitian physics involving strong long-range interactions has been discovered. It leads to pairs of topologically-protected edge states, which exhibit the robust super- or subradiance behavior, localized at the boundaries of the atomic arrays. This work opens an avenue of exploring an interacting quantum optical platform with synthetic dimensions pointing to potential implications for quantum sensing as well as the super-resolution imaging.

The atomic arrays refer to an ensemble of atoms where the interaction of individual atoms and the photon takes place [1]. The light-atom coupling in atomic arrays exhibits fundamental physical phenomena including facilitating the long-range coherent interactions and promoting the collective radiative loss [2]. Recent advances in assembling highly ordered one-dimensional (1D) and two-dimensional (2D) atomic arrays provide unique platforms for exploring the strong light-matter interaction in quantum optics [3–5]. The strong interference in the emitted optical field leads to remarkable optical properties such as the subradiant state [6–8], a high reflection of radiation [9–11], the efficient storage and retrieval for quantum memory [12], and topologically-protected edge states [13, 14], which therefore shows important applications towards quantum information processing, quantum metrology, and nonlinear optics [15].

Topological physics is of fundamental importance where physical characteristics are robust against microscopic variation of system details [16–18]. Topological phenomena can be explored by engineering the Hamiltonian of an atomic or optical system [19–21]. Such approach shows a great potential towards quantum simulation of the topological matter. The topology in atomic or optical systems provides a novel fundamental way of manipulating quantum states of the light, such as robust photon transport in photonic systems [22–25] and non-reciprocal transport in hot atomic gas [26, 27]. Recently, it has been shown that atomic arrays hold a promise for studying topological quantum optics, where the inherent nonlinearity brings a natural way to explore the interacting topological physics [13, 14, 28–30].

Robust single-photon super- and subradiant states hold a significant promise for applications related to quantum storage and quantum information. In this paper, we investigate 1D atomic arrays subjected to a spatially periodic magnetic field. The spatial phase of the magnetic field is an external parameter, and can be used to map one momentum dimension in a 2D system [31, 32]. Therefore, 1D atomic arrays with the synthetic momentum dimension manifests important topological features associated with 2D systems. Systems with synthetic dimensions simplify experimental design and enable capabilities of manipulating atomic quantum states or photons along the synthetic dimension [31–36]. By changing the periodicity of the magnetic field, we show that the 1D atomic arrays exhibit a butterfly-like spectrum, which has not been discussed in the 2D atomic arrays under a uniform magnetic field [13, 28]. Such spectrum, associated with the open quantum optical system involving

long-range interactions along the synthetic dimension, exhibits features, which are dramatically distinct from the spectrum in the 1D photonic model [37, 38]. For a finite 1D atomic arrays, the system supports pairs of topologically-protected boundary states with opposite circularly polarizations, which are found to exhibit super- or subradiance depending on the magnetic field distribution and atomic excitation frequency. The topologically-protected subradiant state localized at the boundary of atomic arrays provides a potential application towards robust quantum storage under the topological protection. The results discussed here show a unique route towards exploring the strong long-range interacting topological physics in quantum optical system with the synthetic dimension.

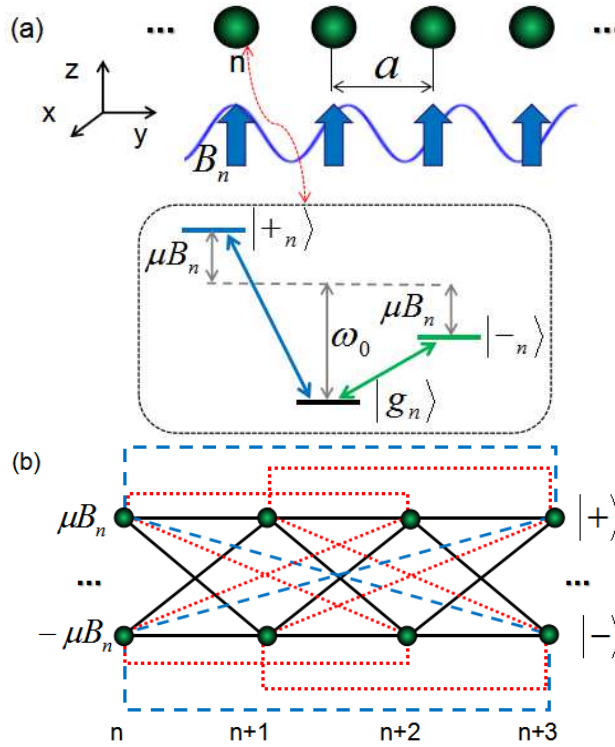


FIG. 1: (a) An 1D atomic arrays subjected to an external spatially periodic magnetic field B_n . Each atom has a V -type atomic level structure with non-degeneracy excited states $|\pm_n\rangle$ split by the magnetic field. (b) The equivalent tight-binding lattice model with on-site potentials $\pm B_n$ and photon-mediated long-range hoppings. Black solid, red dotted and blue dashed lines label the nearest-neighbor, next-nearest-neighbor and triatomic spacing hoppings, respectively, indicating dipole-dipole interactions and collective dissipations.

We propose the experimental arrangement consisting of a 1D arrays of N atoms which are aligned along the y direction with the spacing a . Each atom (labelled by n and located

at y_n) has a V-type internal level structure with the ground state $|g_n\rangle$ and excited states $|\pm_n\rangle = \mp(|x_n\rangle \pm i|y_n\rangle)/\sqrt{2}$, where the transition between $|g_n\rangle$ and $|\pm_n\rangle$ is coupled with the right (left) circularly polarized light. Here $|x(y)\rangle$ refers to the state polarized along the $x(y)$ direction. The degeneracy of the excited states is broken by the presence of an external magnetic field $B_n \equiv B(y_n)$ along the z axis [see Fig. 1(a)].

We consider the dynamics of single-excited atoms coupled to free-space modes of the radiation field. After integrating out radiation modes under the dipole approximation, one obtains the non-Hermitian effective Hamiltonian [11, 13, 28]

$$H = \sum_n \sum_{\alpha=\pm} \left(\omega_0 - i\frac{\gamma_0}{2} + \text{sgn}(\alpha)\mu B_n \right) |\alpha_n\rangle \langle \alpha_n| + \frac{3\pi\gamma_0}{k_0} \sum_{n \neq m} \sum_{\alpha, \beta=\pm} G_{\alpha\beta}(y_n - y_m) |\alpha_n\rangle \langle \beta_m|, \quad (1)$$

where $\omega_0 = k_0 c = 2\pi c/\lambda$ is the atomic transition frequency with the wave vector k_0 and the wavelength λ , γ_0 is the atomic decay rate in the free space, $\text{sgn}(\pm) \equiv \pm$, and μB_n gives the Zeeman shift for the n th atom with the magnetic moment μ . $G_{\alpha\beta}(y_n - y_m)$ is the free-space dyadic Green's function describing the electric field at y_n emitted by the atom located at y_m . By using the Green's function in Cartesian basis [7, 28, 29, 39], one has

$$G_{\pm\pm} = \frac{G_{xx} + G_{yy}}{2} = -\frac{e^{ik_0 r}}{8\pi k_0^2 r^3} (k_0^2 r^2 - ik_0 r + 1), \\ G_{\pm\mp} = \frac{G_{yy} - G_{xx}}{2} = \frac{e^{ik_0 r}}{8\pi k_0^2 r^3} (k_0^2 r^2 + 3ik_0 r - 3), \quad (2)$$

where $r = |y_n - y_m|$.

The atomic system under investigation is an effective tight-binding lattice model [see Fig. 1(b)]. The photon-mediated long-range hoppings amplitude is described by coefficients in the last term of the Hamiltonian, where the real part describes photon-mediated dipole-dipole interaction potential between the n th and m th atoms, while the imaginary part denotes the collective dissipative rate of the two atoms.

To construct the bandstructure of the non-Hermitian Hamiltonian in Eq. (1), we take the linear combination of single-excited states $|\psi\rangle = \sum_n (C_{n,+}|+_n\rangle + C_{n,-}|-_n\rangle)$, where $C_{n,\pm}$ is the amplitude of the wave function for the n th atom with the \pm polarization. The bandstructure can be calculated by using the time-independent Schrödinger equation $H|\psi\rangle = E|\psi\rangle$, which

leads to

$$\begin{aligned}
EC_{n,+} &= \frac{3\pi\gamma_0}{k_0} \sum_{l \neq 0} [G_{++}(la)C_{n+l,+} + G_{+-}(la)C_{n+l,-}] \\
&\quad + (\omega_0 - i\frac{\gamma_0}{2} + \mu B_n)C_{n,+}, \\
EC_{n,-} &= \frac{3\pi\gamma_0}{k_0} \sum_{l \neq 0} [G_{-+}(la)C_{n+l,+} + G_{--}(la)C_{n+l,-}] \\
&\quad + (\omega_0 - i\frac{\gamma_0}{2} - \mu B_n)C_{n,-},
\end{aligned} \tag{3}$$

where l is a nonzero integer. $E \equiv \omega - i\gamma/2$ is the complex eigenvalue, in which ω denotes the self-energy of the collective atomic excitation and γ is the collective decay rate of the system.

We consider a spatially periodic magnetic field

$$B_n = B(y_n) = B_0 \cos(2\pi bn + \phi), \tag{4}$$

where B_0 is the amplitude of the magnetic field, $1/b$ is the spatial period, and ϕ is the modulation phase. By applying the magnetic field with different spatial shapes along the y direction, one has the control of parameters b and ϕ . Here ϕ provides an additional degree of freedom to our system serving the purpose of the synthetic dimension, so the system can be explored by exploiting the parameter-dependency of the Hamiltonian [31, 32]. In such a synthetic space, b gives the effective magnetic flux while ϕ denotes a synthetic momentum dimension (reciprocal to a virtual spatial dimension) [38, 40]. Hence we can study the physics associated to an open 2D system with long-range couplings under the effective magnetic flux.

We plot the projected bandstructure of the system while varying b in Fig. 2. The atomic arrays are assumed to be infinitely long with $a = 0.1\lambda$ and $\mu B_0 = 10\gamma_0$ [13], and bandstructure is computed by following the method in Ref. [41]. One can see a butterfly-like bandstructure (ω), which exhibits multiple bulk bands and gaps for each b . The bandstructure shows several distinguished features as compared to the Hofstadter butterfly bandstructure in Ref. [41] and also the butterfly-like spectrum in the 1D photonic model [37] due to the long-range non-Hermitian couplings in the atomic arrays [42]. The striking feature of our system, as it is seen in Fig. 2, is that the collective decay rate (γ) is changing for different ω at a certain b , covering the range from 0 to $\sim 7.5\gamma_0$. The destructive interference in the atom-photon interaction leads to suppressed radiative loss for certain bulk states as shown in Fig. 2, corresponding to subradiant states with decay rate below the single-atom emission

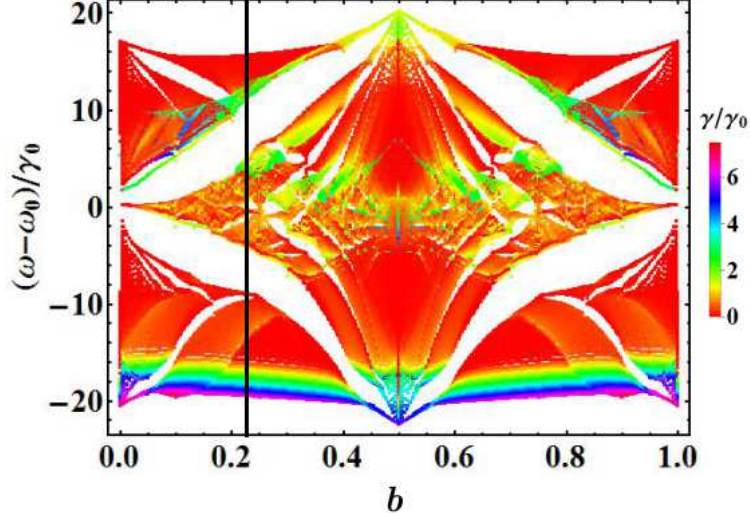


FIG. 2: The numerically calculated projected bandstructure versus b for the infinite 1D atomic arrays with $a = 0.1\lambda$ and $\mu B_0 = 10\gamma_0$. The color of the bandstructure gives the collective decay rate γ .

rate γ_0 . One can therefore control the decay rate to stabilize the quantum coherence in this quantum system.

The parameter b can be externally adjusted by controlling the magnetic field. Once it is irrational, the effective magnetic flux is incommensurate with the lattice and the system exhibits a quasicrystal structure [38]. We set $b = \sqrt{5}/10$, indicated by the black line in Fig. 2. In Fig. 3(a), the bandstructure of the lattice is plotted under an open boundary condition with $N = 101$ against the modulation phase ϕ in the external magnetic field. As a consequence of the presence of the magnetic field which breaks the time-reversal symmetry of the system, the bandstructure is topologically nontrivial. One can see that there is a fractal set of band gaps, and, inside each gap, it exhibits pairs of topologically protected boundary states. The collective decay rates γ for boundary states in two larger gaps show different physical features. The boundary states inside the upper gap has γ greater than γ_0 , corresponding to superradiant modes with enhanced collective emission, while the boundary states inside the lower gap are subradiant because γ is smaller than γ_0 . Moreover, the collective decay rate is also changing along each boundary state when one varies the parameter ϕ , as shown in Fig. 3(b) and 3(c). In particular, for the subradiant boundary states in the lower gap, as indicated in Fig. 3 (c), γ changes from $\sim 0.6\gamma_0$ to $\sim 0.1\gamma_0$, showing a significant suppression of the spontaneous emission. Furthermore, the lifetimes of boundary states are

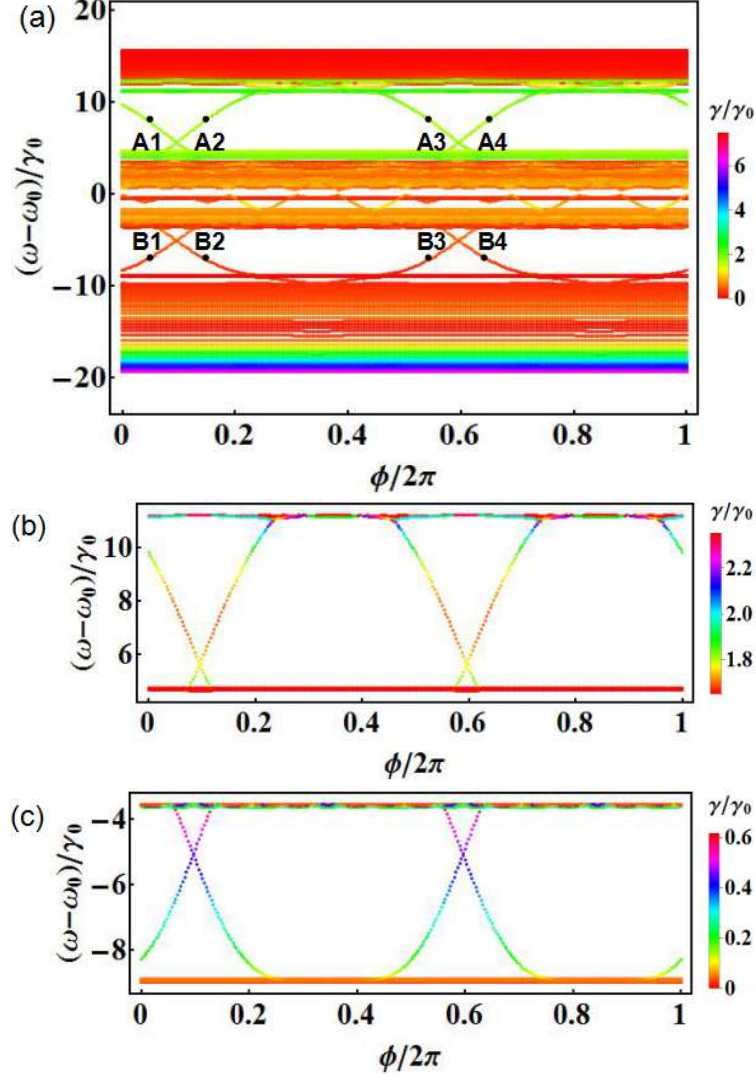


FIG. 3: (a) The bandstructure as a function of ϕ under open boundary condition for atomic number $N = 101$, $a = 0.1\lambda$, $\mu B_0 = 10\gamma_0$ and $b = \sqrt{5}/10$ which corresponds the black line in Fig. 2. (b) and (c) The zoom-in bandstructures from (a), showing the details of boundary states. The color of the bandstructures gives the collective decay rate γ .

influenced by the choice of the parameter b . For instance, for the case $b = (\sqrt{3} - 1)/2$, the boundary states inside the two large gaps are both subradiant as we discuss it in greater details in Supplementary materials [42].

The aforementioned boundary states are localized on the left or right boundary of the lattice with a combination of $|+\rangle$ and $|-\rangle$ excited states. As an example, in Fig. 4, we plot the intensity distributions of boundary states versus the position of the atom n for $|\pm\rangle$

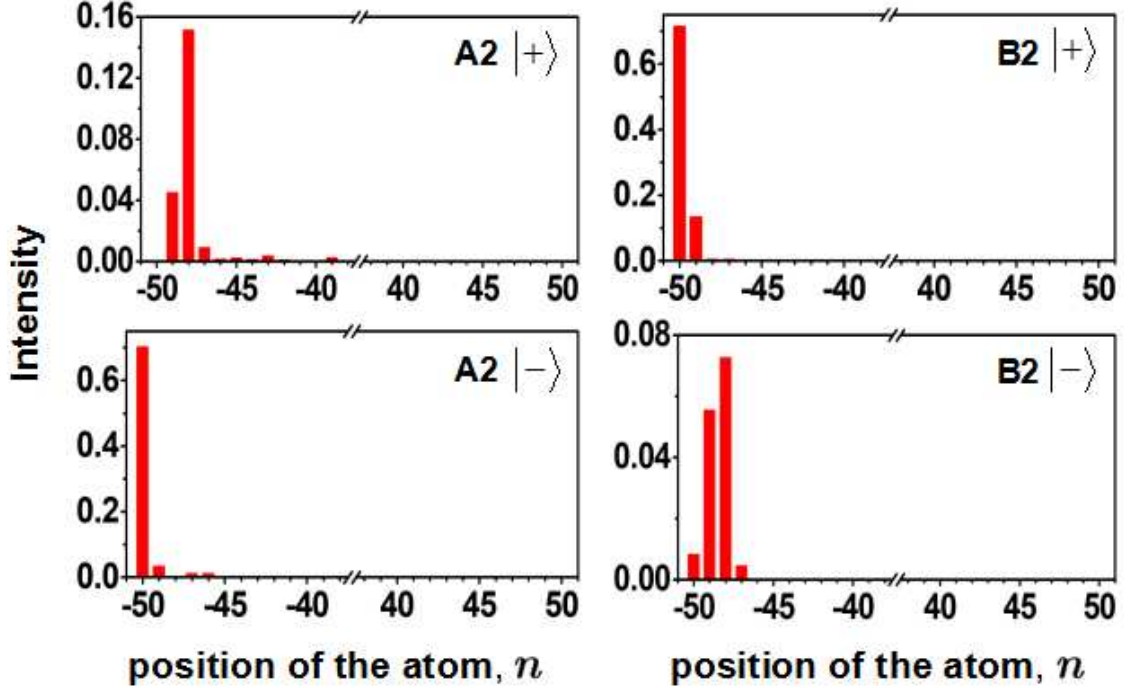


FIG. 4: Intensity distributions of boundary states with $|+\rangle$ (upper row) and $|-\rangle$ (lower row) excited states, labelled by A2 and B2 in Fig. 3(a). Both boundary states are localized on the left boundary of the atomic arrays. A2 and B2 are denoted at $[\phi/2\pi, (\omega - \omega_0)/\gamma_0] = (0.15, 8.15)$ and $(0.15, -7.21)$, respectively.

excited states labelled by A2 and B2 in Fig. 3(a), which corresponds to superradiant and subradiant states, respectively. The superradiant boundary state A2 is located mainly at the $|-\rangle$ excited state on the leftmost atom, while a small portion of the intensity is distributed at $|+\rangle$ on other atoms near the left boundary due to the hoppings between the two excited states on different atoms. We denote the boundary state A2 by $L-$ then. Similarly, the subradiant boundary state B2 is located mainly at the $|+\rangle$ excited state on the leftmost boundary, and hence is labelled by $L+$. The two boundary states corresponding to the same ϕ but different excitation frequency, so one can selectively excite either the superradiant or subradiant boundary states for a given external magnetic fields. Such selectively prepared subradiant state localized at the boundary of the arrays, is robust against small variations of the system due to the topological properties. It therefore shows a potential for the robust quantum storage, which is of great importance for quantum device applications.

Other boundary states labelled by A1, A3, A4 in the upper gap and B1, B3, B4 in the

lower gap, as shown in Fig. 3(a), give R_- (mainly distributed at $|-\rangle$ on the right boundary), R_+ (mainly distributed at $|+\rangle$ on the right boundary), L_+ and R_+ , R_- , L_- , respectively. One therefore can selectively prepare a super- or subradiant state with either right or left circularly polarization by a choice of ϕ . In each gap, the boundary states located at the same boundary with opposite polarization excitations exhibit propagating modes toward the same direction along the virtual spatial dimension (reciprocal to the synthetic momentum dimension ϕ), while the boundary states at different boundaries support propagating modes towards opposite direction.

The proposed system is experimentally feasible. For example, an atomic array with the subwavelength-scale lattice spacing can be realized by using bosonic strontium [43, 44]. The transition between triplet states 3P_0 and 3D_1 of atom ^{84}Sr gives emission at the wavelength $\lambda = 2.6\mu\text{m}$. One can use the optical lattice formed by lasers at 412.8nm to trap the atoms, which achieves a subwavelength lattice spacing $a = 206.4\text{nm}$, i.e., $a/\lambda \approx 0.08$ [43]. Inhomogeneous magnetic field is widely used to produce spin-orbit couplings in the condensed matter systems [45, 46]. The magnetic field in Eq. (4) can be implemented by a variety of experimental technologies which have been proposed to construct magnetic lattices [47–51]. One can use a circularly polarized laser at a frequency resonant with the boundary state L_{\pm} (R_{\pm}) inside the band gap to excite the $|\pm\rangle$ state of the atom located at the left (right) boundary. The emission of such super- or subradiant boundary state is localized at the boundary of atomic arrays with the enhanced or suppressed collective decay rate.

In summary, we have investigated 1D atomic arrays subjected to the spatially periodic magnetic field, which supports the non-Hermitian lattice model with long-range interactions. The phase in the magnetic field serves as an external parameter, which gives a synthetic momentum dimension. In atomic arrays with strong long-range interactions, the bulk-boundary correspondence is not generally valid [14]. In the open system proposed here, we consider a synthetic space including one spatial dimension and one synthetic momentum dimension. By carefully selecting parameters, we show the existence of the 2D bulk-boundary correspondence in this synthetic space that exhibits topologically-protected boundary states, which holds fundamentally different physics from the 1D atomic arrays with a non-zero Zak phase [29]. These boundary states are localized at the boundary of atomic arrays and exhibit topologically-protected super- or subradiance with right or left circularly polarization. Our results show potential applications towards manipulating atomic emission at the single pho-

ton level under the topological protection, which is important for the quantum memory and quantum information, and also leads potential implications for quantum sensors [52, 53] and super-resolution spectroscopy [54] by using the robust single-photon superradiant states. The study of topological quantum optics with synthetic dimensions opens a route of exploring topological phenomena in versatile higher-dimensional strong-interacting open quantum systems.

Acknowledgments

This paper is supported by the National Nature Science Foundation of China (NSFC) No. 11734011 and the National Key R&D Program of China (2017YFA0303701).

-
- [1] W. E. Lamb, J. and R. C. Retherford, Phys. Rev. **72**, 241 (1947).
 - [2] R. Dicke, Phys. Rev. **93**, 99 (1954).
 - [3] T. Xia, M. Lichtman, K. Maller, A. W. Carr, M. J. Piotrowicz, L. Isenhower, and M. Saffman, Phys. Rev. Lett. **114**, 100503 (2015).
 - [4] M. Endres, H. Bernien, A. Keesling, H. Levine, E. R. Anschuetz, A. Krajenbrink, C. Senko, V. Vuletic, M. Greiner, and M. D. Lukin, Science **354**, 1024 (2016).
 - [5] D. Barredo, S. de Léséleuc, V. Lienhard, T. Lahaye, and A. Browaeys, Science **354**, 1021 (2016).
 - [6] G. Facchinetti, S. D. Jenkins, and J. Ruostekoski, Phys. Rev. Lett. **117**, 243601 (2016).
 - [7] A. Asenjo-Garcia, M. Moreno-Cardoner, A. Albrecht, H. J. Kimble, and D. E. Chang, Phys. Rev. X **7**, 031024 (2017).
 - [8] P.-O. Guimond, A. Grankin, D. V. Vasilyev, B. Vermersch, and P. Zoller, Phys. Rev. Lett. **122**, 093601 (2019).
 - [9] F. J. García De Abajo, Rev. Mod. Phys. **79**, 1267 (2007).
 - [10] R. J. Bettles, S. A. Gardiner, and C. S. Adams, Phys. Rev. Lett. **116**, 103602 (2016).
 - [11] E. Shahmoon, D. S. Wild, M. D. Lukin, and S. F. Yelin, Phys. Rev. Lett. **118**, 113601 (2017).
 - [12] M. T. Manzoni, M. Moreno-Cardoner, A. Asenjo-Garcia, J. V. Porto, A. V. Gorshkov, and D. E. Chang, New J. Phys. **20**, 083048 (2018).

- [13] J. Perczel, J. Borregaard, D. E. Chang, H. Pichler, S. F. Yelin, P. Zoller, and M. D. Lukin, *Phys. Rev. Lett.* **119**, 023603 (2017).
- [14] R. J. Bettles, J. Minář, C. S. Adams, I. Lesanovsky, and B. Olmos, *Phys. Rev. A* **96**, 041603(R) (2017).
- [15] K. Hammerer, A. S. Sørensen, and E. S. Polzik, *Rev. Mod. Phys.* **82**, 1041 (2010).
- [16] K. V. Klitzing, G. Dorda, and M. Pepper, *Phys. Rev. Lett.* **45**, 494 (1980).
- [17] D. C. Tsui, H. L. Stormer, and A. C. Gossard, *Phys. Rev. Lett.* **48**, 1559 (1982).
- [18] R. B. Laughlin, *Phys. Rev. Lett.* **50**, 1395 (1983).
- [19] T. Ozawa, H. M. Price, A. Amo, N. Goldman, M. Hafezi, L. Lu, M. C. Rechtsman, D. Schuster, J. Simon, O. Zilberberg, and I. Carusotto, *Rev. Mod. Phys.* **91**, 015006 (2019).
- [20] N. R. Cooper, J. Dalibard, and I. B. Spielman, *Rev. Mod. Phys.* **91**, 015005 (2019).
- [21] D.-W. Zhang, Y.-Q. Zhu, Y. X. Zhao, H. Yan, and S.-L. Zhu, *Advances in Physics*, **67**, 253 (2019).
- [22] Z. Wang, Y. Chong, J. D. Joannopoulos, and M. Soljačić, *Nature* **461**, 772 (2009).
- [23] M. Hafezi, E. Demler, M. Lukin, J. Taylor, *Nat. Phys.* **7**, 907 (2011).
- [24] K. Fang, Z. Yu, S. Fan, *Nat. Photon.* **6**, 782 (2012).
- [25] M. C. Rechtsman, J. M. Zeuner, Y. Plotnik, Y. Lumer, D. Podolsky, F. Dreisow, S. Nolte, M. Segev, and A. Szameit, *Nature* **496**, 196 (2013).
- [26] D.-W. Wang, H. Cai, L. Yan, S.-Y. Zhu, R.-B. Liu, *Optica* **2**, 712 (2015).
- [27] H. Cai, J. Liu, J. Wu, Y. He, S.-Y. Zhu, J.-X. Zhang, D.-W. Wang, *Phys. Rev. Lett.* **122**, 023601 (2019).
- [28] J. Perczel, J. Borregaard, D. E. Chang, H. Pichler, S. F. Yelin, P. Zoller, and M. D. Lukin, *Phys. Rev. A* **96**, 063801 (2017).
- [29] B. X. Wang and C. Y. Zhao, *Phys. Rev. A* **98**, 023808 (2018).
- [30] J. Perczel, J. Borregaard, D. E. Chang, S. F. Yelin, M. D. Lukin, arXiv:1810.12299 (2018).
- [31] L. Yuan, Q. Lin, M. Xiao, and S. Fan, *Optica* **5**, 1396 (2018).
- [32] T. Ozawa and H. M. Price, *Nat. Rev. Phys.* (2019). DOI: 10.1038/s42254-019-0045-3.
- [33] M. Lohse, C. Schweizer, H. M. Price, O. Zilberberg, and I. Bloch, *Nature* **553**, 55 (2018).
- [34] O. Zilberberg, S. Huang, J. Guglielmon, M. Wang, K. P. Chen, Y. E. Kraus, and M. C. Rechtsman, *Nature* **553**, 59 (2018).
- [35] E. Lustig, S. Weimann, Y. Plotnik, Y. Lumer, M. A. Bandres, A. Szameit, and M. Segev,

- Nature **567**, 356 (2019).
- [36] A. Dutt, M. Minkov, Q. Lin, L. Yuan, D. A. B. Miller, and S. Fan, arxiv.org/abs/1903.07842.
 - [37] L. Lang, X. Cai, and S. Chen, Phys. Rev. Lett. **108**, 220401 (2012).
 - [38] Y. E. Kraus, Y. Lahini, Z. Ringel, M. Verbin, and O. Zilberberg, Phys. Rev. Lett. **109**, 106402 (2012).
 - [39] O. Morice, Y. Castin, and J. Dalibard, Phys. Rev. A **51**, 3896 (1995).
 - [40] C. Shang, X. Chen, W. Luo, and F. Ye, Opt. Lett. **43**, 275 (2018).
 - [41] D. R. Hofstadter, Phys. Rev. B **14**, 2239 (1976).
 - [42] See the Supplemental Materials.
 - [43] B. Olmos, D. Yu, Y. Singh, F. Schreck, K. Bongs, and I. Lesanovsky, Phys. Rev. Lett. **110**, 143602 (2013).
 - [44] S. V. Syzranov, M. L. Wall, V. Gurarie, and A. M. Rey, Nat. Commun. **7**, 13543 (2016).
 - [45] Y. Tokura, W. G. van der Wiel, T. Obata, and S. Tarucha, Phys. Rev. Lett. **96**, 047202 (2006).
 - [46] M. Pioro-Ladrière, T. Obata, Y. Tokura, Y.-S. Shin, T. Kubo, K. Yoshida, T. Taniyama, and S. Tarucha, Nat. Phys. **4**, 776 (2008).
 - [47] A. D. West, K. J. Weatherill, T. J. Hayward, P. W. Fry, T. Schrefl, M. R. J. Gibbs, C. S. Adams, D. A. Allwood, and I. G. Hughes, Nano Lett. **12**, 4065 (2012).
 - [48] B. M. Anderson, I. B. Spielman, and G. Juzeliūnas, Phys. Rev. Lett. **111**, 125301 (2013).
 - [49] X. Luo, L. Wu, J. Chen, R. Lu, R. Wang, and L. You, New J. Phys. **17**, 083048 (2015).
 - [50] Y. Wang, P. Surendran, S. Jose, T. Tran, I. Herrera, S. Whitlock, R. McLean, A. Sidorov, and P. Hannaford, Sci. Bull. **61**, 1097 (2016).
 - [51] J. Yu, Z. Xu, R. Lü, and L. You, Phys. Rev. Lett. **116**, 143003 (2016).
 - [52] J. Kitching, S. Knappe, and E. A. Donley, IEEE Sens. J. **11**, 1749 (2011).
 - [53] S. J. Roof, K. J. Kemp, and M. D. Havey, Phys. Rev. Lett. **117**, 073003 (2016).
 - [54] A. von Diezmann, Y. Shechtman, and W. E. Moerner, Chem. Rev. **117** 7244 (2017).